Author/s:
Zhang, B;Gao, C;Neto, NS;Wong, WWH

Title:
Aggregation-induced emitters in light harvesting

Date:
2019

Citation:
Zhang, B., Gao, C., Neto, N. S. & Wong, W. W. H. (2019). Aggregation-induced emitters in light harvesting. Tang, Y (Ed.). Tang, BZ (Ed.). Principles and Applications of Aggregation-Induced Emission, (1st), pp.479-504. Springer.

Persistent Link:
https://hdl.handle.net/11343/344894

Aggregation-induced Emitters in Light Harvesting

Bolong Zhang, Can Gao, Nicolau Saker Neto and Wallace W. H. Wong

1. Introduction

The manipulation and use of sunlight can be traced back to Romans and Greeks in the 3rd century B.C. who used mirrors to concentrate solar energy to light torches.[1] The first solar collector, the 'hot box', was invented by Swiss scientist Horace de Saussure in 1767 and then later was improved and used for practical food cooking in 1803.[2] In 1816, Robert Stirling invited a heat engine that concentrated solar thermal energy and generated electricity.[3] French scientist Edmond Becquerel discovered the photovoltaic effect in 1839[4] and American inventor Charles Fritts made the first solar cells from selenium wafers in 1883.[5] In 1954, Daryl Chapin, Calvin Fuller, and Gerald Pearson developed the silicon photovoltaic (PV) cell at Bell Labs.[6] The development of humankind is strongly tied to solar energy with continuous development of technologies of solar light harvesting.

In addition to understanding fundamental scientific processes and creating better device architectures, the development of novel materials is an essential aspect in enabling next-generation solar light harvesting technologies. Advances in solar PV technologies provide great examples of this combined approach.[7] Apart from converting solar energy to electrical current in PV technologies, materials for other types of light harvesting devices, such as artificial photosynthesis[8] and photon refining, are in development to enhance energy transfer and photon-to-photon conversion efficiency.

Among all light harvesting materials, aggregation-induced emission (AIE) type chromophores[9] show unique photophysical[8] properties required in many light harvesting technologies. In general, common chromophores usually suffer aggregation-caused quenching (ACQ) that decreases the photoluminescent quantum yield (Φ_{PL}) of chromophores as a function of the increasing molecular aggregation level. However, in aggregation-induced emitters, chromophore aggregates instead show enhanced Φ_{PL}. By virtue of the AIE effect, some of these materials can be used in different fields of light harvesting that require high PL quantum efficiency, good energy transfer efficiency and high concentration quenching tolerance of their chromophores. Benefiting from many photophysical properties of AIE-type materials, new technologies and applications in different aspects of both artificial photosynthesis and photon refining have been developed. Notably, although many classic AIE-type molecular building blocks are used in organic PV materials, they do not generally make use of the AIE effect[10] and, therefore, will not be discussed in this chapter.

In this chapter, we will describe the criteria of AIE-type chromophores required in the fields of light harvesting. Following, the applications of AIE chromophores in artificial photosynthesis and photon refining will be discussed in detail.

2. Artificial photosynthesis

Photosynthesis describes the process in which the energy of solar light is captured and stored by an organism, and the stored energy is used to drive energy-requiring cellular processes.[8c, 11] Photosynthesis converts solar energy into chemical energy (Figure 1a). There are four phases in a typical natural photosynthetic process, namely the energy collection, primary photochemistry, stabilization by secondary reactions and the synthesis of stable products. Although the detailed photosynthetic mechanism may differ between species, most of them start with the solar light being absorbed by a type of protein complex called light-harvesting antenna complex.[12] This complex usually consists of proteins and light-harvesting pigments that surround the photosynthetic reaction center (Figure 1).[13] The entire system is called a photosynthesis unit. The light-harvesting antenna is essential as energy from multiple photons is required to drive reactions at the reaction centre. Once the light is absorbed by the pigments located on the antenna complex, the energy transfers through different pigment molecules, in a process called energy migration, to the photosynthetic reacting center, where the water splitting reaction then occurs. The produced chemical energy is temporarily stored in adenosine triphosphate (ATP) and later in glucose.

The light-harvesting antenna component of photosynthesis is remarkably efficient given the number of pigments involved. Both the energy cascade and the spatial arrangement of the chromophores should be ideally established to allow energy to funnel efficiently to the reaction centre. It is therefore a great challenge to mimic photosynthesis in this respect in artificial photosynthetic systems. To better understand how to design new light harvesting materials, a critical aspect to consider is the mechanism of energy transfer in light-harvesting arrays.

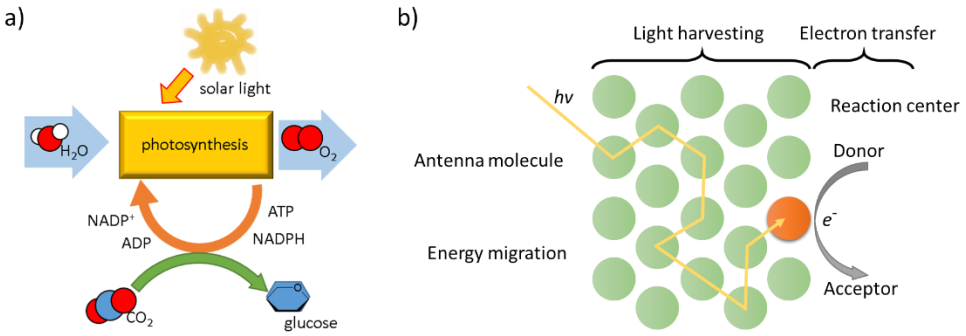

Figure 1 Simple illustration of a) the photosynthesis process and b) the energy migration in light-harvesting antennae.

Looking more closely at the energy transfer processes in natural photosynthesis, the light-harvesting antenna system containing many chromophore molecules surrounds the reaction center acting as an energy funnel. Once a photon is captured, the energy has to be transferred via a large number of chromophores before reaching the reaction center. This energy transfer process can proceed through a variety and combination of mechanisms, including Förster resonance energy transfer (FRET), Dexter energy transfer, exciton coupling and quantum coherence, depending on the molecular distance, orientations and the photophysical properties of the chromophores. Among them, the FRET approach is one of the most observed energy

transfer process in photosynthesis and has been well studied from many aspects.[11b, 14] In general, to allow the exciton hopping, FRET process requires the appropriate alignment of energy levels of the energy-donating and the energy-accepting molecules. The overlap of transition dipoles of the molecules is also necessary for energy transfer via FRET. However with correct energy level alignment and relative molecular orientation, FRET allows relatively long through-space energy transfer distances in the nanometer range. The FRET critical radius (R_0, nm) refers to the molecular distance where the efficiency of FRET is 50%. R_0 is defined via the following Förster equation:[15]

$$R_0 = 0.02108 \times \left(\frac{\kappa^2 \Phi_{PL} J}{n^4}\right)^{\frac{1}{6}}$$

$$J = \int \varepsilon_A(\lambda) F_D(\lambda) \lambda^4 \, d\lambda$$

where κ^2 is the orientation factor (κ^2=2/3 for a randomly-oriented long lifetime donor-acceptor system), Φ_{PL} refers to the photoluminescent quantum efficiency of the donor chromophore in the absence of the acceptor, J(nm^{4}M^{-1}cm^{-1}) is a coefficient of the energy levels overlap which can be calculated from the overlap between the normalized (area) emission spectrum (F_D) of the donor and the extinction coefficient (ε_A) of the acceptor, λ is the wavelength over the full spectrum, and n stands for the refractive index of the matrix material. It is worth mentioning that this equation can describe both single and multi-chromophore systems. According to the above equation, the FRET process is highly dependent on the donor-to-acceptor energy levels overlap (J), Φ_{PL} of chromophores and the concentration of the chromophores (average molecular distance should be smaller than R_0). The overlap of the energy levels can be easily tuned via varying the donor or acceptor chromophores.

One way to improve the efficiency of energy migration in artificial photosynthesis is to build a chromophore architecture system that is ideal for the FRET process.[16] AIE-type chromophores show the benefit of high Φ_{PL} in high concentration or aggregated state. As efficient energy transfers via FRET typically require average separation in the sub-nanometer range, the ability to use higher concentrations of chromophores or dye aggregates while maintaining high Φ_{PL} is a clear advantage. One example in the literature made use of the self-assembly of an amphiphilic AIE chromophore to create highly fluorescent vesicles.[16] In this research, the authors designed and synthesized two tetraphenylethylene (TPE) derivatives with bile acid substituents capable of self-assembly in appropriate solvents (Figure 2). The vesicles were highly emissive due to the AIE phenomenon of the TPE moieties in the architecture. The authors then inserted two guest dyes, Nile red (hydrophobic) and rhodamine B (hydrophilic), into the amphiphilic binding pockets. The FRET efficiency from TPE in the vesicle was 52.4% to Nile red and 41.8% to rhodamine B. Similar results were observed in both monolayer and bilayer vesicle systems. All results indicated the binding pockets provided the required orientation for the inserted molecules to transfer energy with the TPE shell via the FRET process. This research provides a new approach for self-assembling host-guest artificial light harvesting complexes.

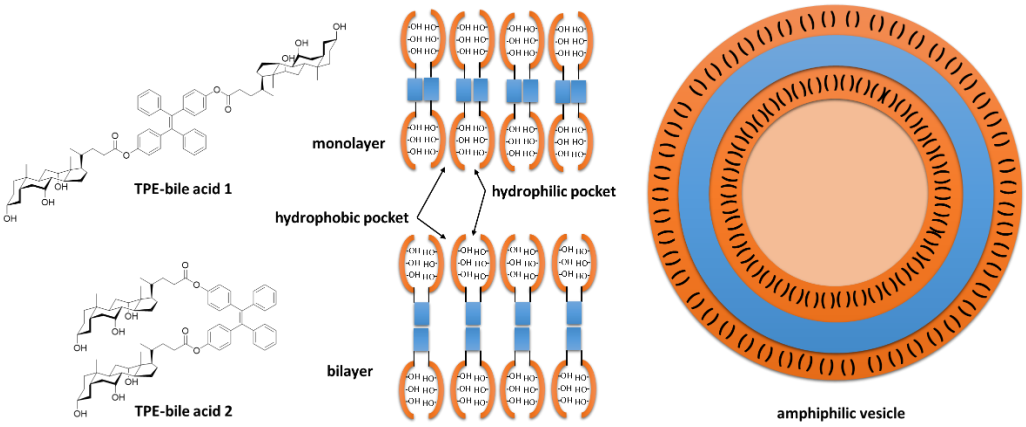

Figure 2 The amphiphilic vesicle self-assembled from either monolayer or bilayer structures based on TPE-bile acid 1 and TPE-bile acid 2. Both the hydrophobic and hydrophilic pockets are embedded on the surfaces of the vesicle.

A series of poly(amidoamine) (PAMAM) based dendrimers with TPE chromophore as the dendritic peripheral substituents provides another example of an AIE-type light harvesting array (Figure 3).[17] When dissolved in toluene, the dendrimer D4 was highly emissive while the TPE model building block was dark. The emission intensity of D4 was independent of the concentration, indicating the emission was a result of intramolecular aggregation. By switching the solvent from toluene to THF or chloroform, which increased the solubility of the dendrimer backbone, the emission intensity of all dendrimers decreased. Better solvation of the material led to extension of the dendrimer branches and hence more flexibility and freedom of motion for the TPE moieties, making the material less emissive. Furthermore, the emission efficiency of the material changed with temperature. The extension and contraction of the dendrimer structure with stimuli was referred to as the 'breathing' behaviour of material. This responsiveness of the material can be considered as mimicking natural photosynthesis light harvesting systems. There are further reported examples of dendrimers showing AIE behaviour that are not specifically designed for light harvesting.[18]

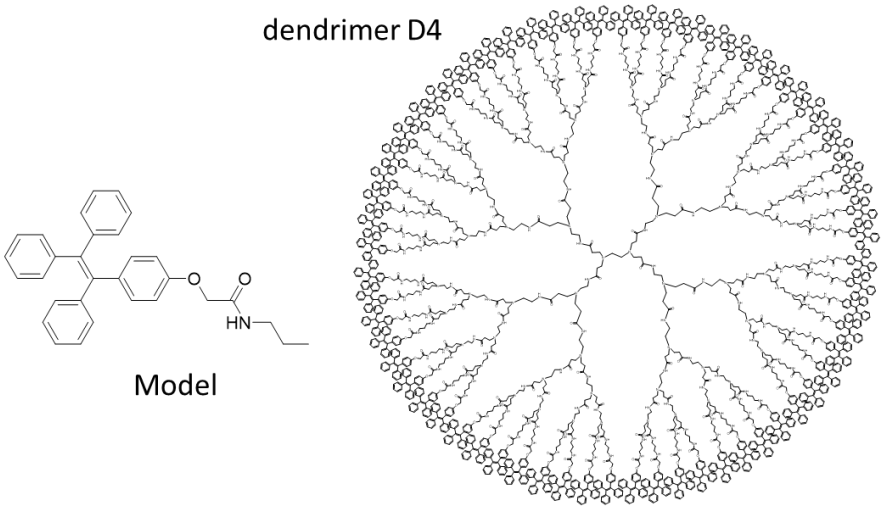

Figure 3 The chemical structure of the Model and the dendrimer D4.

Another example of an array of AIE chromophores is a functional conjugated microporous polymer (CMP) based on the TPE moiety.[19] Unlike metal organic frameworks (MOFs) and covalent organic frameworks (COFs), the structure of CMPs are usually formed kinetically and lack long-range periodicity (Figure 4). This reported CMP consisted of TPE cores covalently linked by diethynylbiphenyl bridges to form the three-dimensional framework. Both the CO_2 storage ability and the light harvesting performance of this microporous CMP were demonstrated. The CMP was very emissive in the solid state. Like many AIE chromophores, the emission turned on when the free rotation of the substituents on the chromophore was restricted. For the CMP material, the rotational restriction stemmed from the rigidity and covalent links within the three-dimensional framework. Furthermore, the small molecule chromophore rhodamine B (RhB) was introduced into the microporous CMP framework as an acceptor dye. The absorption spectrum of RhB significantly overlapped with the emission spectrum of the CMP material, and the emission of the RhB@CMP complex suggested an efficient energy transfer from the CMP framework to RhB. Inspired by the strong emission features and inherent microporosity, the RhB@CMP complex provided an ideal platform for light-harvesting antennae based on the AIE-type donor-acceptor system.

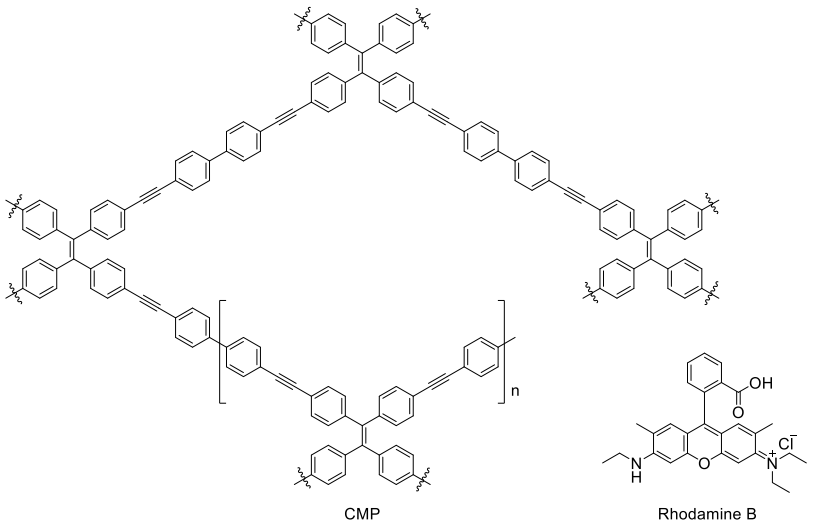

Figure 4 The molecular structure of covalent organic framework CMP and Rhodamine dye RhB.

A self-assembling system based on sulfato-β-cyclodextrin (SCD), an AIE-type chromophore oligo(phenylenevinylene) derivative (OPV-1) and the fluorescent dye Nile red was examined in light harvesting for artificial photosynthesis (Figure 5). OPV-1 formed emissive aggregates in aqueous solution but the emission was enhanced by the addition of cyclodextrin SCD which promoted the self-aggregation of aromatic or amphiphilic molecules. The critical aggregation concentration of OPV-1 was lowered by the cyclodextrin forming aggregates with greater emission intensity. At the molecular ratio of 1:6, SCD and OPV-1 self-assembled into multilayer nanoparticles with diameter ranging from 50 to 150 nm. Energy transfer was observed from OPV-1 to Nile red when Nile red was loaded into the SCD/OPV-1 nanoparticles. At the OPV-1 to Nile red ratio of 125:1, the donor-to-acceptor FRET process efficiency was 72% and the antenna efficiency was 32%.

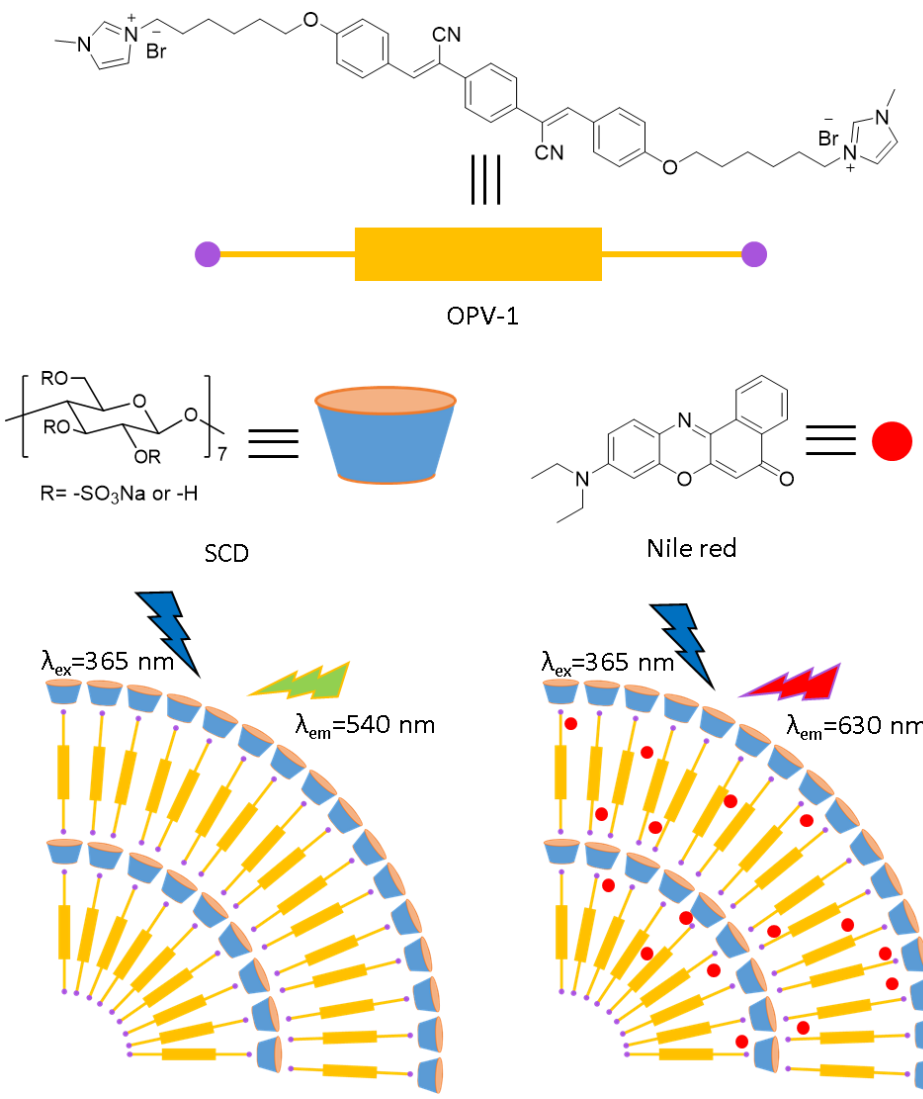

Figure 5 The chemical structures of OPV-1, cyclodextrin SCD and Nile red The self-assembled multilayer nanoparticles emit at 540 nm. After doping with Nile red, the emission redshifts to 630 nm.

As a further example of supramolecular AIE-type materials used to mimic photosynthesis light-harvesting antenna complexes, an assembly between cucurbit[8]uril (CB[8]) and naphthyl-substituted AIE-type fluorophore moieties (TPE and 9,10-bis((E)-2-(pyridin-4-yl) vinyl)anthracene) in aqueous solution has been reported (Figure 6a).[20] The host-guest complexation structures of CB[8] restricted the free rotation of the substituents in the AIE-fluorophores, and therefore led to strongly emissive complexes even in dilute dispersions. Another study showed a host-guest complex based on TPE derivatives (M1) and boron-dipyrromethane (M2) donor-acceptor dye system (Figure 6b).[21] The association of M1 and M2 positioned the TPE and boron-dipyrromethane chromophores closer together enabling FRET to occur.

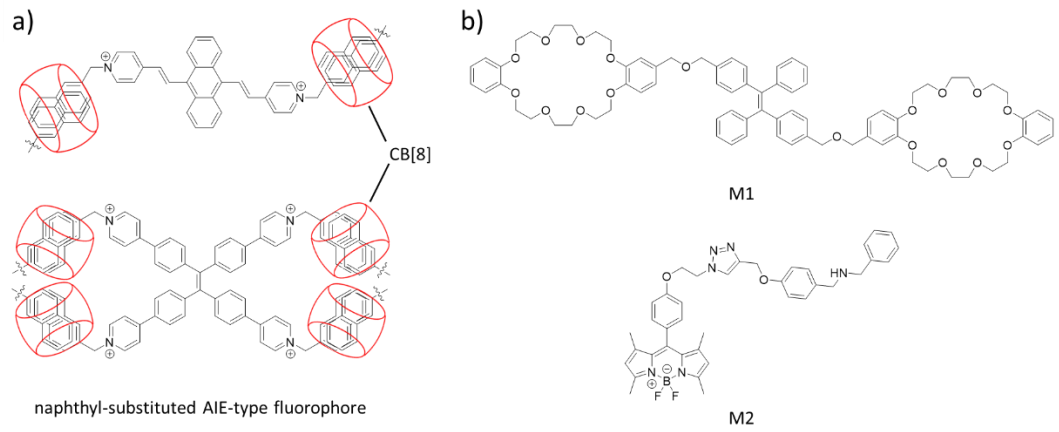

Figure 6 a) The supramolecular host-guest complexes formed by CB[8] and naphthyl-substituted AIE-type fluorophores; b) the chemical structures of the host M1 and the guest M2.

The examples in this section show the advantage of using AIE-type chromophores in light-harvesting arrays. While it is clear that chromophores that do not display AIE behaviour, as with natural photosynthetic pigments, can be used for light harvesting, AIE-type emissive aggregates offer greater versatility and less stringent spatial control of the chromophores.

3. Photon refining

Photon refining can be defined as a process in which photons are manipulated for a desired application. Light concentration, spectral wavelength tuning, photon energy fusion and photon energy fission are all processes of photon refinement.[22] In the context of light harvesting, photon refining is used to improve energy conversion efficiency which has a direct impact on reducing cost of energy generation.

For photovoltaics, photon refining provides approaches to overcome the Shockley-Quiesser efficiency limit (SQ limit). The SQ limit is defined as the maximum theoretical efficiency of a single p-n junction photovoltaic cell under one sun irradiation.[23] Photon refining can address two key aspects of this SQ limit – sunlight intensity and the bandgap of the photoactive semiconductor.

Light concentration can be easily achieved by focusing light into a small area typically through the use of mirrors. While it is clear how light concentration works in solar thermal applications, its effect on photovoltaics is less obvious at first glance. The primary effect of light concentration on photovoltaic efficiency comes from increases in the device voltage with increasing light intensity.[24] The level of efficiency improvement is modulated by power losses to heat stemming from the series resistance of the device. Light concentration can also be achieved using waveguides in combination with luminescent materials. These luminescent waveguide devices, otherwise known as luminescent solar concentrators (LSCs), will be discussed in the next section.

A single p-n junction photovoltaic cell has a fundamental efficiency limit because of the amount of light energy that can be converted given the bandgap of the semiconductor (Figure 7). For photons of short wavelength, the photon energy is much higher than the bandgap of the material, which leads to energy loss by thermal relaxation. On the other hand, photons at long wavelength go unused because the photon energy is less than the bandgap of the photovoltaic material.

Therefore, according to the SQ limit, the power conversion efficiency for single junction solar cells cannot exceed 33.7%. To overcome this limitation, photon refining techniques such as multi-exciton generation and photon upconversion can be applied to make better use of high energy and below-bandgap photons, respectively, and improve the total power conversion efficiency of the photovoltaic devices.

In the next section, the application of AIE-type materials in solar concentrator and photon upconversion devices will be reviewed and discussed.

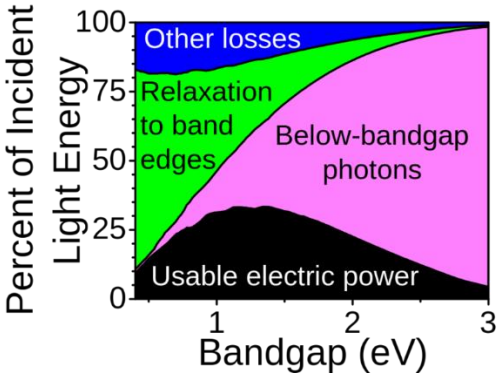

Figure 7 A diagram of the Shockley-Queisser limit. The maximum efficiency of a traditional solar cell (black) under one-sun condition (AM 1.5) and the energy losses in percentage of the incident light energy against the band gap (or energy gap) of the solar cell materials.[25]

3.1 Luminescent solar concentrator (LSC)

A luminescent solar concentrator (LSC) is a device that can harvest solar light in a large area and concentrate the re-emitted light to a relatively smaller area.[26] A typical LSC device consists of a planar transparent waveguide, made of glass or plastic, containing photoluminescent materials. The photoluminescent materials capture the incident photons and the emitted photons are trapped in the waveguide by total internal reflection. In this way, light is waveguided to the edge of the device leading to concentration of light at the edge. This concentrated light can then be converted to electric current by photovoltaic cells attached on the LSC device edge.[27] The performance of an LSC is defined by the energy loss mechanisms in the device which can be divided into two main categories: losses stemming from the photophysical properties of the chromophore (to be discussed in detail in the following sections); and waveguide losses which include reflection, scattering and escape cone loss (Figure 8a). The first LSC devices can be traced back to as early as 1951 with a report of a planar fluorescence collecting system designed for radiance amplification (a radiation sensor).[28] In 1976,[29] a planar solar collector was reported using a medium containing chromophores to harvest light and a solar cell to collect the emission via total internal reflection. Subsequent improvements on this prototype include a multi-dye planar solar concentrator.[30] In the latter work, a donor dye was used to harvest light and transfer the energy to an acceptor dye which had an emission window matched to the absorbance spectrum of the photovoltaic cell.

A variety of LSC device geometries exist especially when one includes devices integrated with photovoltaics.[26a] Here, two basic LSC geometries are presented with relevance to following discussions.[26a, 31] One is called bulk-doped LSC, which consists of a single piece of waveguide (usually polymer matrix) with luminescent dyes dispersed homogenously inside the matrix (Figure 8). The other is called thin-film LSC, which is made of a clear waveguide with a thin layer of dye-containing plastic matrix casted on top (Figure 8). The key difference between these two LSC device geometries is the concentration of chromophore required to achieve the desired level of light harvesting. Thin-film LSCs require higher concentration of the chromophore to achieve the same absorbance compared to thick bulk-doped devices, but they have some advantages in device fabrication. Depending on the chromophore, it is sometimes a challenge to fabricate bulk-doped LSCs with uniform dye dispersion.

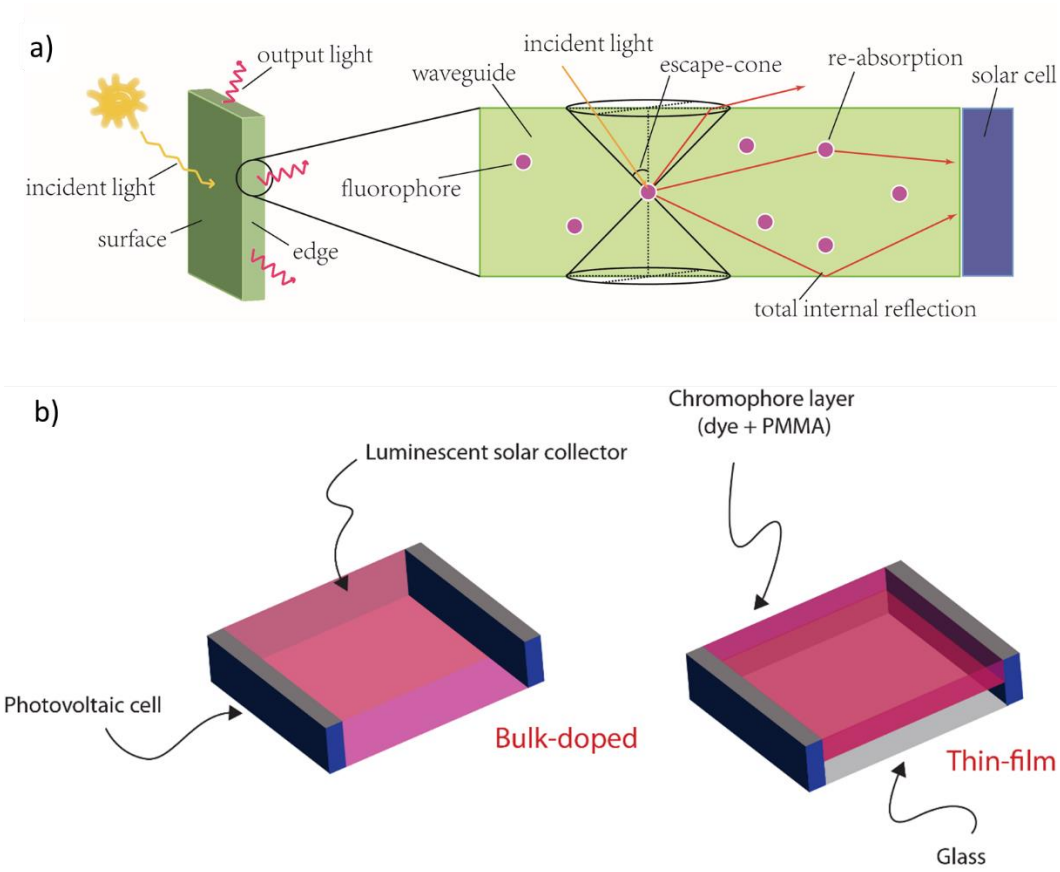

Figure 8 a) The schematic diagram of a typical LSC device and b) the general structures of bulk-doped LSC and thin-film LSC devices. The waveguide matrix of bulk-doped LSC is usually made of plastics, so the chromophores can be pre-blended into the matrix materials and dispersed homogeneously in the waveguide system. The thin-film LSC is usually made of glass plates which are coated with a thin chromophore-embedded plastic membrane.

There are several advantages to using LSCs as a light harvesting device.

1. LSCs are excellent at harvesting diffuse light.
2. The materials used to construct an LSC can be very cheap, reducing the cost of photovoltaics by reducing the required photovoltaic cell area.

3. The planar and potentially light-weight device geometry allows easy integration in applications, such as building-integrated photovoltaics.
4. The device geometry is such that the photovoltaic cells are unlikely to suffer from overheating, as can be the case in mirror-type concentrators.
5. LSC devices are less bulky compared to mirror-type concentrators.

There are of course problems and challenges in improving LSC performance.

1. The state-of-the-art efficiency of light trapping can be improved by using more advanced dye systems.
2. Coupled with good waveguide optical properties, the maximum light concentration (flux gain) should scale appropriately with device size (geometric gain).
3. There are some long term device stability challenges.

The following section contains definition of some key LSC device performance parameters to consider. The geometric gain, *G*, is a factor describing the ratio of surface area to edge area in LSC devices:

$$G = \frac{S_{surface}}{S_{edge}}$$

where S_{edge} and $S_{surface}$ are the area of the edges and surface of the waveguide respectively. By using LSC with large geometric gain, one is able to significantly reduce the photovoltaic cell area required per unit of light harvesting area from $S_{surface}$ to S_{edge}. How LSC performance scales with *G* will be an important factor in building-integrated devices, particularly transparent LSCs used as windows.[26a]

The ability of an LSC to concentrate light is measured by the flux gain, *F*, and is defined as the intensity of light emitted at the edges of the LSC device divided by the incident light intensity (see equation below). Flux gain can be used to determine the external quantum efficiency (EQE) of the device of certain size or geometric gain.

$$F = \frac{I_{edge}}{I_{surface}} = EQE \times G$$

$$EQE = \frac{n_{edge}}{n_{incident}}$$

where I_{edge} refers to the intensity of one edge output and $I_{surface}$ is the flux incident on the surface. n_{edge} is the number of the total edge output photons and $n_{incident}$ is number of the incident photons to the surface. It is important to note that the wavelengths at which the LSC operates can be tuned by variation of the chromophore. This means it is possible to match LSC wavelength with photovoltaic cell bandgap. This tunability is not apparent from the device performance parameters given above.

To maximise the performance of an LSC device, the choice of chromophore is critical.[32] LSC chromophores are required to have:

- Good photo- and thermal stability.
- High molar absorptivity to collect photons as efficiently as possible.
- High Φ_{PL} in the medium of the LSC, typically poly(methyl methacrylate) (PMMA) matrix.
- Separation between the absorption and emission band of the chromophore (Stokes shift) to avoid re-absorption of emission.

The latter two requirements will be addressed in the section below.

High chromophore $\boldsymbol{\Phi_{PL}}$ *in LSC devices*

A large portion of chromophores reported in LSC devices are commercially available dyes, though there is increasing number of reports on new organic dye structures, luminescent polymers and quantum dots.[26a, 32a, 33] Typical luminescent organic dyes (e.g. coumarins, rhodamines, perylenes, etc.) have planar aromatic structures and are prone to self-aggregation resulting in the aggregation-caused quenching (ACQ) of photoluminescence. Although dyes are dispersed in polymer matrices in LSC devices, these organic dyes will still aggregate with increasing concentration as they do in solution. This means dye concentration must remain low to maintain high Φ_{PL} and, as a consequence, thicker devices are necessary to maintain good absorbance. AIE-type chromophores have a clear advantage over typical organic dyes in this application. AIE chromophores are not only emissive in their aggregated state but also when dispersed in a solid-state matrix.[9b, 9c, 34]

It has been demonstrated that TPE is highly photoluminescent in polystyrene matrix.[35] Interestingly, TPE was more emissive in glassy polystyrene compared to poly(styrene-butadiene) copolymer. It was suggested that the rotational motion of the phenyl groups of the TPE was more restricted in the rigid glassy matrix making the sample more emissive. TPE has also been examined in LSC devices.[36] In a proof-of-concept study, a series of phenyl-substituted alkene compounds were investigated as potential LSC chromophores. While all compounds in the study showed AIE behaviour, their Φ_{PL} was lower than the simple TPE structure. Subsequently, the performance of TPE in LSCs was tested as a thin film on glass showing Φ_{PL} of 49.5% and n_{edge} of 13.7% at *G* = 50. The large 1.1 eV Stokes shift of TPE meant that re-absorption of emission was small and the performance of TPE devices scaled well with area. The topics of Stokes shift and re-absorption are discussed in greater detail in the next section. One problem identified with TPE was its crystallinity as opaque light-scattering films were obtained when TPE was used in high concentration in PMMA. This highlights the importance of physical compatibility of the dye with the waveguiding matrix. TPE is a UV-absorbing material with emission in the blue region. While suitable for transparent device applications such as smart windows, LSC devices containing TPE have limited power output as it does not harvest any visible light.

A red-emitting AIE-type chromophore, TPE-AC, has been reported for a visible light harvesting LSC.[37] The LSC devices were fabricated by dispersing TPE-AC in PMMA in chloroform solution and coated on top of glass substrates. Evaporation of the solvent resulted in PMMA thin films 25±5 µm thick embedded with TPE-AC. The prepared TPE-AC films had wavelength of maximum emission in the 600 - 620 nm range and the maximum Φ_{PL} was 50% with 0.1 wt% of dye in the

polymer matrix. The Φ_{PL} decreased to 30% with 1.2 wt% of TPE-AC in PMMA. Interestingly, polycarbonate films containing TPE-AC showed higher Φ_{PL} at greater dye concentration. The Φ_{PL} of the TPE-AC/polymer film at the highest chromophore content were comparable to benchmark materials at long wavelength range.[38] The observed optical quantum efficiency maximum of TPE-AC LSC devices was 6.7%, comparable to other reported LSCs with red-emitting chromophores.[39] Following this research, the same group reported a TPE-substituted red-emitting ATRP initiator that can be used in PMMA-based LSC devices.[40] The TPE-substituted chromophore shows excellent photostability but the Φ_{PL} requires improvement to increase LSC performance.

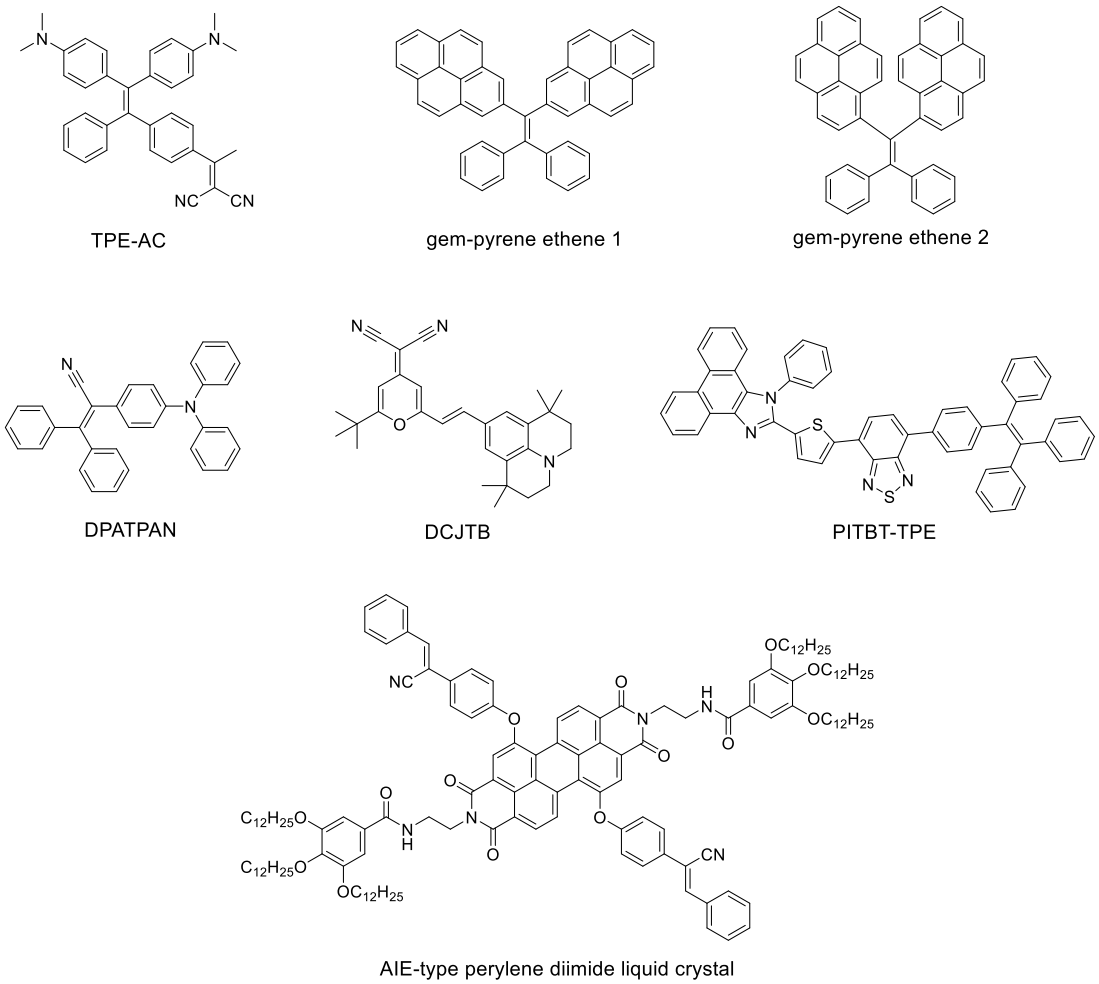

Figure 9 The chemical structure of AIE-type chromophores and laser dye DCJTB used in LSC devices.

It is important to note that while the photoluminescence properties of AIE-type chromophores are advantageous for LSCs as described above, other classes of dyes that show high solid-state Φ_{PL} can also lead to efficient devices. This includes molecularly insulated chromophores and other emissive aggregates.[32b, 32c]

Chromophores with large Stokes shift

The Stokes shift is another key criterion for chromophores used in LSCs as it has a large impact on

the re-absorption of emission leading to energy loss. The re-absorption effect of LSCs refers to the process in which light emitted from one chromophore is absorbed by other chromophore molecules in the device. Re-absorption does not directly cause any energy loss, however, losses can occur when chromophores excited by the re-absorbed photons undergo non-radiative decay or the re-emitted light escapes through the escape cone of the waveguide (Figure 8). The severity of the re-absorption effect in a waveguide system is based on three factors, namely the absorption and emission spectra overlap of the chromophores (a higher Stokes shift suggests a smaller overlap), the concentration of chromophores and also the geometric size of the waveguide. In most cases, the last two factors are determined by other design criteria of the specific LSC application. Therefore, eliminating the spectral overlap of the chromophores is the main approach to address the re-absorption effect. By increasing the total Stokes shift of the dyes chosen in LSC devices, the chance for re-absorption in LSC waveguide systems can be reduced. Two major strategies have been used to increase the total Stokes shift of chromophores used in LSCs, both with relevance to the photophysical properties of AIE-type chromophores.

The most straightforward approach is choosing chromophores that already have very large Stokes shifts, a requirement met by some AIE-type materials.[41] As described earlier, the classic AIE chromophore, TPE, has been reported in a proof-of-principle LSC device.[36] While TPE shows a high Stokes shift of 130 nm, the lower Φ_{PL} results in LSC devices with moderate performance. An advancement on this work was reported with two gem-pyrene ethene derivatives providing even larger Stokes shifts (Figure 9).[42] Both molecules showed AIE effect in solution and in polystyrene matrix, but gem-pyrene ethene 2 showed higher Φ_{PL} up to 64%. Interestingly, the Stokes shift of ethene 1 was about 60 nm, while the Stokes shift of pyrene 2 was significantly increased to 180 nm. The emission spectrum of pyrene 2 was significantly redshifted and was indicative of excimer formation and emission. Crystallographic data for pyrene 2 showed crystal packing of pyrene dimers that are well-known to form excimers on photoexcitation. The combination of good Φ_{PL} and large Stokes shift for pyrene 2 makes it an appropriate chromophore for a transparent LSC device.

Although not specifically designed for LSC application, another example of an AIE-type material showing large Stokes shift is an intramolecular energy donor-acceptor system (Figure 9).[43] The molecule consisted of cyanoethene groups attached to the bay position of a liquid crystalline perylene diimide. When excited at 330 nm, where the cyanoethene substituent absorbs, the energy transferred to the perylene core and the molecule emitted at 575 nm, resulting in a large Stokes shift of 251 nm. Notably, the Φ_{PL} of the material increased as a function of the increasing ratio of H_2O in THF/H_2O solution, which indicated the AIE effect. Further research regarding intramolecular donor-acceptor system based on AIE-type functional substituents has been reported in recent years.[44]

Donor-acceptor FRET pair

Combinations of dyes with matching absorption and emission energies have been used to improve LSC performance.[45] Using multiple chromophores can increase spectral coverage of LSCs as well as reduce emission re-absorption.[32b] To reduce re-absorption, the approach is to use a blend of at least two chromophores that can form a donor-acceptor FRET pair. The donor dye molecules are usually the dominant species in order to capture the incident light, while the

acceptors are used in a much smaller amount in order to minimize the spectral overlap (Figure 10). Once the incident light is absorbed by the donor, the excited molecules transfer the energy to the acceptors via the FRET process and the acceptors re-emit the light. Therefore, the overall spectrum of the blend reveals mainly the donor's absorption and the acceptor's emission spectra and leads to an increased total Stokes shift. This donor-acceptor blend approach provides a constructive method to modify both the absorption and emission spectra of LSC devices. However, it requires a high concentration of the chromophores to provide efficient energy transfer process with average intermolecular distance of no more than a few nanometers for efficient FRET process. Therefore, this approach should only be used in thin-film LSC devices and most chromophores which undergo the ACQ effect are not applicable.

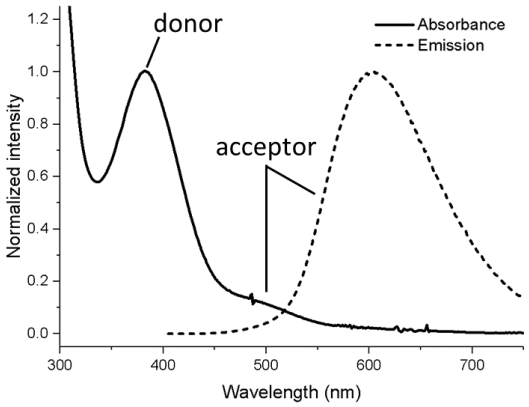

Figure 10 An example of the donor-acceptor blend to improve the overall Stokes shift.[16]

AIE-type materials have recently been used to pursue the donor-acceptor blend approach. An AIE energy donor, DPATPAN, was used with a commercially available laser dye, DCJTB, as the energy acceptor and emitter in LSC devices (Figure 9).[34b] DPATPAN is a typical AIE material which showed >90% Φ_{PL} in PMMA matrix when dilute (less than 10% w/w) and still maintained close to 90% Φ_{PL} at high concentration (50% w/w). On the other hand, the acceptor DCJTB is a typical organic dye that shows the ACQ effect, with unity Φ_{PL} at low concentration and rapidly decreasing Φ_{PL} at increasing concentration (80% Φ_{PL} at 1% w/w in PMMA). It was demonstrated that, at the donor-acceptor molar ratio of 99:1, the emission of the donor was fully quenched by the acceptor. The overall Φ_{PL} of the chromophore blend remained at above 90% while the Stokes shift increased from about 50 nm to 190 nm.

A pair of AIE chromophores, DPATPAN and PITBT-TPE, has also been investigated in LSC devices (Figure 9).[46] Limited by the poor photo-stability in air and the ACQ effect, the LSC devices based on DCJTB were unstable and high concentrations could not be achieved. To overcome these problems, PITBT-TPE was introduced as an alternate acceptor. In PMMA matrix, PITBT-TPE reached almost 90% Φ_{PL} in low concentration, while still maintaining 45% Φ_{PL} at a concentration of 225 mM. The emission of DPATPAN (250 mM) was fully quenched with 22.5 mM PITBT-TPE, which indicated the high efficiency of the FRET process from DPATPAN to PITBT-TPE. The re-absorption effect in the LSC based on the donor-acceptor blend was reduced in comparison with LSC based on pure donor material, which lead to an increase in the optical quantum efficiency of the LSCs with the donor-acceptor blend.

AIE-type chromophores show good Φ_{PL} in solid-state plastic matrix and improve the concentration tolerance to the ACQ effect, which perfectly fits the needs of LSC devices. Some AIE-type chromophores show relatively large Stokes shifts, while others show energy transfer ability in donor-acceptor blend systems. Both cases show benefits in reducing the re-absorption effect and make AIE-type chromophores more competitive candidates in LSCs. Above all, the AIE-type materials provide new strategies in designing and fabricating LSC devices.

3.2 Photon Upconversion

Photon upconversion is an anti-Stokes shift process taking low energy light to generate higher energy light. As discussed in the introductory photon refinement section, this phenomenon is particularly useful for improving the performance of photovoltaic devices with the fixed bandgap of the semiconducting material. Sub-bandgap photons normally go unused in photovoltaics.[47] Therefore, any process that allows the use of those photons will improve photovoltaic device performance.

There are three types of photon upconversion processes. Perhaps the most well-known and studied process is two-photon absorption process in which near-simultaneous absorption of two coherent photons is needed. This process requires the use of coherent, high intensity excitation by pulsed high power lasers. This means two-photon absorption is unsuitable for solar light harvesting.[48] Two alternative photon upconversion pathways have been devised for achieving upconversion under continuous wave low energy excitation; (i) lanthanide-based upconversion and (ii) triplet-triplet annihilation upconversion. The former depends on the f-electron configurations of lanthanide ions to facilitate absorption of multiple photons and generate upconverted luminescence emission.[49] Triplet-triplet annihilation photon upconversion (TTA-UC) is a promising route as tunable organic chromophores are involved and it has been demonstrated to operate with moderate excitation power.[50] The sections below summarise the TTA-UC mechanism and discuss reported dye systems involving AIE materials.

TTA-UC mechanism

TTA-UC is a bimolecular process requiring two chromophores, a sensitizer and an emitter. It is based on the anti-Stokes delayed fluorescence first reported by Parke and Hatchard in the 1960s.[51] The mechanism of the TTA-UC process is as follows (Figure 11). A sensitizer (donor) molecule absorbs lower energy photons and is excited to its first singlet excited state ($^1S \rightarrow {}^1S^*$). Subsequently the sensitizer undergoes efficient intersystem crossing (ISC) forming the corresponding triplet excited state ($^3S^*$). The energy stored in the sensitizer's triplet excited state is rapidly and efficiently transferred to the emitter (acceptor) through triplet-triplet energy transfer (TTET), forming a triplet species ($^3E^*$). Two emitter triplets then collide and produce one emitter in its ground state (^1E) and one singlet excited state ($^1E^*$). Finally, the excited singlet state decays radiatively to the ground state by fluorescence and releases a photon of higher energy than that of the individual photons initially absorbed.[52]

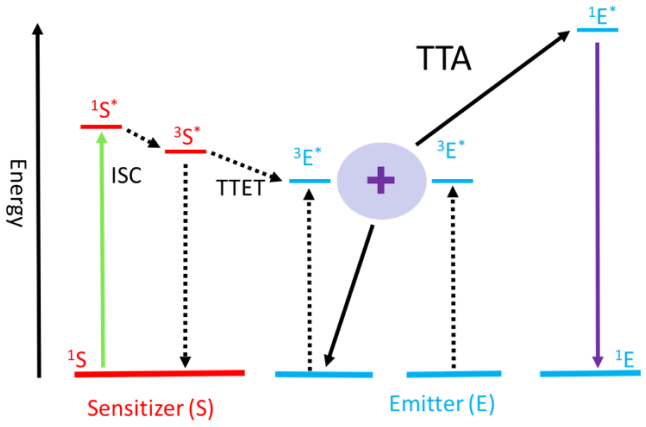

Figure 11 Working mechanism of TTA-UC.

Selection of chromophores for TTA-UC

The upconversion wavelengths of TTA-UC are highly tunable, depending on the choice of sensitizer-emitter chromophore pair. The chromophores used for TTA-UC have specific requirements. For the sensitizer, the requirements are as follows:[52]

1. Strong absorption in the desired absorption region.
2. High intersystem crossing yield (Φ_{ISC}~ 1).
3. Long triplet lifetime (>10 μs) to facilitate efficient diffusional-dependent triplet energy transfer to the emitter.
4. Small singlet-triplet gap to minimize energy loss in the process of ISC.

The emitter species have different requirements to the sensitizer, namely:

1. A singlet state at just below double the energy of the first triplet in order to make TTA energetically favorable.
2. High photoluminescence quantum yield (Φ_{PL} ~ 1).
3. First triplet state ($T_{1,E}$) energy close to, but slightly lower than, that of the triplet energy of sensitizer ($T_{1,S}$).

TTA-UC efficiency

In addition to the individual properties of the sensitizers and emitters, the overall quantum efficiency of the TTA-UC (Φ_{UC}) is a product of events involved in the upconversion mechanism, and is expressed by the following:[53]

$$\Phi_{UC} = \frac{1}{2} f \Phi_{ISC} \Phi_{ET} \Phi_{TTA} \Phi_{PL}$$

where Φ_{ISC} is the ISC quantum yield of the sensitizer, Φ_{ET} is the TTET quantum efficiency from the sensitizer in its triplet excited state to the emitter, Φ_{TTA} is the TTA quantum efficiency between two emitters in their triplet excited states, and Φ_{PL} is the fluorescence quantum yield of the emitter. The factor ½ originates from the stoichiometry of the TTA upconversion process in which two excited triplets are required to generate one higher energy singlet excited state, thus the maximum upconversion quantum yield is 50%. Lastly, f represents the statistical probability

of obtaining the singlet state after annihilation of two excited triplet states.

According to the above equation, to achieve high upconversion quantum yield, Φ_{ISC}, Φ_{ET}, Φ_{TTA}, Φ_{PL} are the key factors to be considered. The terms Φ_{ISC} and Φ_{PL} mainly depend on the properties of the chromophores, therefore, the selection of chromophores is critical to yield efficient TTA-UC. The Φ_{ET} and Φ_{TTA} parameters are largely dependent on external factors, such as molecular diffusion, triplet excited state concentration and incident power density. Each individual step involved in the TTA upconversion should be optimized to maximize the overall upconversion efficiency.

AIE materials for TTA-UC

To date, efficient TTA-UC has been achieved in solution phase due to the fast triplet molecular diffusion in solution, which is essential for the TTET and TTA processes. However, the use of volatile organic solvents and overwhelming deactivation of excited triplet states by dissolved oxygen severely hamper their real-world applications. Therefore, significant effort has been devoted to developing solid state TTA-UC systems. Unlike many organic chromophores, molecules which exhibit AIE behaviour do not suffer from concentration quenching in the aggregated state. This aspect of AIE materials is very attractive for TTA-UC applications, particularly in solid-state devices. Solid-state TTA-UC requires high chromophore concentration to achieve high Φ_{ET} and Φ_{TTA} while maintaining Φ_{PL}. AIE materials have been observed to maintain high Φ_{PL} even in high concentration or as a neat film.[9c] Aggregation of molecules also means the chromophores are closely packed together, which has the potential to enhance both Φ_{ET} and Φ_{TTA} leading to overall more efficient TTA-UC.

An aggregation-induced TTA-UC system has been reported with well-known AIE chromophore, cyano-substituted oligo(p-phenylenevinylene) (CN-OPV), and Pt(II) octaethyl-porphyrin (PtOEP) used as the emitter and triplet sensitizer respectively (Figure 12).[54] When the sensitizer-emitter blend was excited in solution at 532 nm, the TTA-UC emission was not observed. However, the TTA-UC emission was observed when the blend was in an aggregated state. In solution, the substituents around the vinylene group in CN-OPV can rotate freely after sensitization. In the twisted configuration, the energy gap between the T_1 and S_0 states of compound is small enough to allow T_1-to-S_0 intersystem crossing, which then leads to deactivation instead of TTA-UC. By restricting the molecular configuration in the solid state, the conformation of CN-OPV was fixed and the triplet excited state was not deactivated. Further, the triplet excitons could then migrate through the crystalline CN-OPV domain. When two triplet excitons met in the crystal, triplet-triplet annihilation was observed followed by emission from the newly-created singlet exciton. Furthermore, the study showed that the alignment of CN-OPV was improved upon doping with PtOEP and it was possible to achieve better aggregation-induced TTA-UC by properly tuning the interaction between the sensitizer and the emitter.

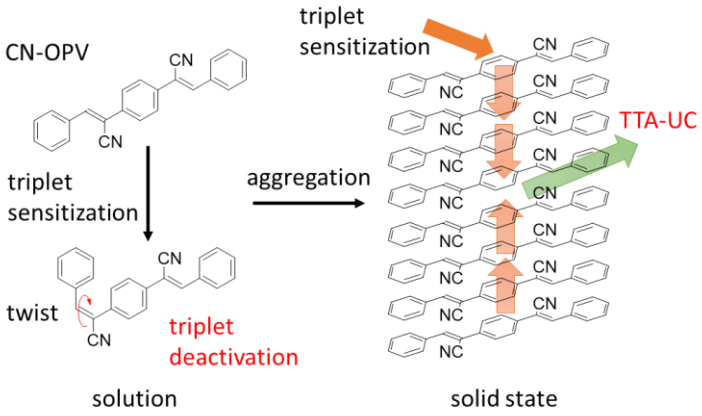

Figure 12 Illustration of the process of aggregation-induced TTA-UC. In solution, the triplet sensitization of CN-OPV causes the rotation of substituents around the C=C bond and leads to the triplet energy loss by fast non-radiative decay. In solid state or aggregate form, the conformation of CN-OPV is locked. The triplet excitons then migrate through the aligned chromophores, promoting the TTA-UC process.

The phase separation of sensitizer and emitter blends is a significant problem for solid-state TTA-UC devices. Advancement in this area was made by modifying the sensitizer and an AIE-type emitter with glutamate-based self-assembling moieties in an aggregation-induced TTA-UC system (Figure 13).[55] In general, both the TTET and TTA processes occur via the Dexter energy transfer process, which requires very short intermolecular distances (less than 1 nm) between the materials and good overlap of the wavefunctions. The self-assembly of both the sensitizer and the emitter provided the possibility to solve this problem by binding the molecules a short distance apart and fixing the wavefunctions in a favourable orientation. The chiral emitter material L-1 reported in this research could self-assemble into organogels when dispersed in a variety of solvents. This was attributed to intermolecular hydrogen bonding on the amide groups on the two ends of the molecule. The emission spectra of the emitter material redshifted with increasing polarity of the solvent from toluene to DMF. L-1 showed a gelation-induced enhancement of emission, an AIE phenomenon. By decreasing the temperature of the solution from 90 ^{o}C to ambient, the authors observed a blueshift and photoluminescence intensity increase. To co-assemble the supramolecular sensitizer and emitter blend, PtOEP linked with the glutamate-based self-assembling moieties L-2 was prepared. The binary donor-acceptor gel was formed in toluene with L-2 molecularly dispersed within the self-assembling L-1 gel structure. The aggregation-induced TTA-UC of the binary L-1/L-2 self-assembling gel was affected by the degree of gelation, evidenced by the observed UC emission at room temperature and its disappearance at 90 ^{o}C. In this research, the combined concept of aggregation-induced TTA-UC and molecular self-assembly was successfully demonstrated in a thermally switchable TTA-UC system.

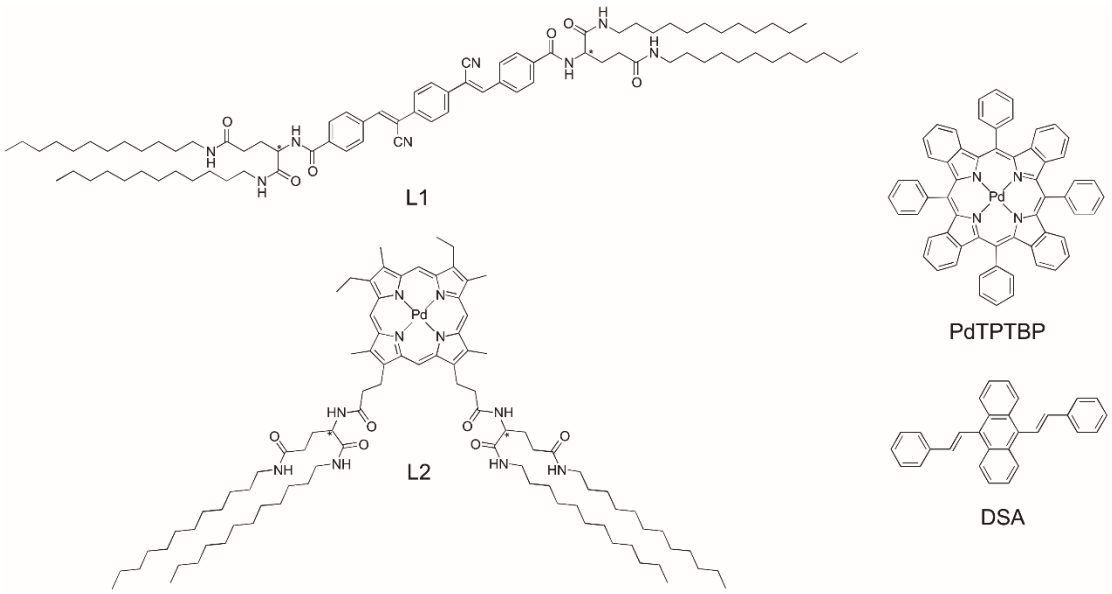

Figure 13 Chemical structures of emitter L-1 and sensitizerL-2, porphyrin sensitizer PdTPTBP and anthracene emitter DSA.

A nanocrystal system showing AIE effect has also been examined for TTA-UC (Figure 13).[56] This reported UC system was based on nanocrystals of an AIE-type emitter, 9,10-distyrylanthracene (DSA) and palladium(II) meso-tetraphenyltetrabenzoporphyrin (PdTPTBP) as sensitizer. When a mixture of PdTPTBP and DSA (1:800) in solution was excited at 640 nm, the triplet-triplet energy transfer was close to unity but there was no upconverted emission observed. The authors then prepared the sensitizer-emitter blend nanocrystal by precipitating PdTPTBP and DSA solution (THF, 1:800) in sodium dodecyl sulfate aqueous solution. When excited at 640 nm, the sensitizer-emitter blend nanocrystal powder showed upconverted emission at 514 nm with the TTA-UC efficiency about 0.29%.

Molecules with AIE properties show high fluorescence quantum yield in solid state and rigid frameworks or environmental effects can be introduced into the AIE systems to extend the triplet lifetime. The TTA upconversion by triplet energy migration and annihilation by using AIE molecules provides a promising way to achieve solid-state upconversion, which is the ideal system for photovoltaic applications.

The examples of reported research in this chapter clearly show the role of AIE materials in light harvesting. In general, light harvesting systems aim to achieve maximum photon conversion efficiency. In this respect, AIE materials provide two key advantages: minimising the energy loss via non-radiative decay from excited states, and as a consequence maximising photoluminescence quantum yield in aggregated form; and enabling close proximity of chromophores to allow efficient energy transfer. It is anticipated that AIE materials and tunable dye aggregate systems will continue to have significant impact in the areas of artificial photosynthesis and photon refining.

References:

(1) The History of Solar. Available at: https://www1.eere.energy.gov/solar/pdfs/solar_timeline.pdf (Accessed 27 February 2018).

(2) Horace de Saussure and his hot boxes of the 1700's. Available at: http://www.solarcooking.org/saussure.htm (Accessed 27 February 2018).

(3) Stirling Engines: History 1816-1937. Available at: http://sesusa.org/history.1816.htm (Accessed 27 February 2018).

(4) Becquerel, A.-E., *CR Acad. Sci.* **1839,** *9* (145), 1.

(5) Fritts, C. E., *Am. J. Sci.* **1883,** (156), 465-472.

(6) Chapin, D. M.; Fuller, C. S.; Pearson, G. L. Solar energy converting apparatus. US Patent 2780765A, 1957.

(7) (a) Antonanzas, J.; Osorio, N.; Escobar, R.; Urraca, R.; Martinez-de-Pison, F. J.; Antonanzas-Torres, F., *Solar Energy* **2016,** *136*, 78-111; (b) Gratzel, M., *Nature* **2001,** *414* (6861), 338-44.

(8) (a) Arp, T. B.; Barlas, Y.; Aji, V.; Gabor, N. M., *Nano Lett.* **2016,** *16* (12), 7461-7466; (b) Berardi, S.; Drouet, S.; Francas, L.; Gimbert-Surinach, C.; Guttentag, M.; Richmond, C.; Stoll, T.; Llobet, A., *Chem. Soc. Rev.* **2014,** *43* (22), 7501-19; (c) Scholes, G. D.; Fleming, G. R.; Olaya-Castro, A.; van Grondelle, R., *Nat. Chem.* **2011,** *3* (10), 763-74.

(9) (a) Hong, Y.; Lam, J. W.; Tang, B. Z., *Chem. Soc. Rev.* **2011,** *40* (11), 5361-88; (b) Mei, J.; Hong, Y.; Lam, J. W.; Qin, A.; Tang, Y.; Tang, B. Z., *Adv. Mater.* **2014,** *26* (31), 5429-79; (c) Mei, J.; Leung, N. L.; Kwok, R. T.; Lam, J. W.; Tang, B. Z., *Chem. Rev.* **2015,** *115* (21), 11718-940.

(10) (a) Liu, Y.; Mu, C.; Jiang, K.; Zhao, J.; Li, Y.; Zhang, L.; Li, Z.; Lai, J. Y.; Hu, H.; Ma, T.; Hu, R.; Yu, D.; Huang, X.; Tang, B. Z.; Yan, H., *Adv. Mater.* **2015,** *27* (6), 1015-20; (b) Rananaware, A.; Gupta, A.; Li, J.; Bilic, A.; Jones, L.; Bhargava, S.; Bhosale, S. V., *Chem. Commun.* **2016,** *52* (55), 8522-5; (c) Shi, J.; Huang, J.; Tang, R.; Chai, Z.; Hua, J.; Qin, J.; Li, Q.; Li, Z., *Eur. J. Org. Chem.* **2012,** *2012* (27), 5248-5255.

(11) (a) Lambers, H.; Chapin, F. S.; Pons, T. L., Photosynthesis. In *Plant Physiological Ecology*, Springer New York: New York, NY, 2008; pp 11-99; (b) Blankenship, R. E., *Molecular mechanisms of photosynthesis*. John Wiley & Sons: 2014.

(12) Herek, J. L.; Wohlleben, W.; Cogdell, R. J.; Zeidler, D.; Motzkus, M., *Nature* **2002,** *417* (6888), 533-5.

(13) Mirkovic, T.; Ostroumov, E. E.; Anna, J. M.; van Grondelle, R.; Govindjee; Scholes, G. D., *Chem. Rev.* **2017,** *117* (2), 249-293.

(14) Frischmann, P. D.; Mahata, K.; Wurthner, F., *Chem. Soc. Rev.* **2013,** *42* (4), 1847-70.

(15) (a) Demchenko, A. P., Fluorescence Detection Techniques. In *Introduction to Fluorescence Sensing*, 2009; pp 65-118; (b) Medintz, I.; Hildebrandt, N., *FRET-Förster resonance energy transfer: from theory to applications* **2013**.

(16) Zhang, M.; Yin, X.; Tian, T.; Liang, Y.; Li, W.; Lan, Y.; Li, J.; Zhou, M.; Ju, Y.; Li, G., *Chem. Commun.*

2015, *51* (50), 10210-3.

(17) Zeng, Y.; Li, P.; Liu, X.; Yu, T.; Chen, J.; Yang, G.; Li, Y., *Polym. Chem.* **2014,** *5* (20), 5978-5984.

(18) (a) Lv, Q.; Liu, M.; Wang, K.; Mao, L.; Xu, D.; Zeng, G.; Liang, S.; Deng, F.; Zhang, X.; Wei, Y., *J. Taiwan Inst. Chem. E.* **2017,** *75*, 292-298; (b) Arseneault, M.; Leung, N. L. C.; Fung, L. T.; Hu, R.; Morin, J.-F.; Tang, B. Z., *Polym. Chem.* **2014,** *5* (20), 6087-6096.

(19) Suresh, V. M.; Bonakala, S.; Roy, S.; Balasubramanian, S.; Maji, T. K., *J. Phys. Chem. C* **2014,** *118* (42), 24369-24376.

(20) (a) Qiao, F.; Zhang, L.; Lian, Z.; Yuan, Z.; Yan, C.-Y.; Zhuo, S.; Zhou, Z.-Y.; Xing, L.-B., *J. Photochem. Photobiol., A* **2018,** *355*, 419-424; (b) Qiao, F.; Yuan, Z.; Lian, Z.; Yan, C.-Y.; Zhuo, S.; Zhou, Z.-Y.; Xing, L.-B., *Dyes Pigm.* **2017,** *146*, 392-397.

(21) Wang, S.; Ye, J.-H.; Han, Z.; Fan, Z.; Wang, C.; Mu, C.; Zhang, W.; He, W., *RSC Adv.* **2017,** *7* (57), 36021-36025.

(22) McKenna, B.; Evans, R. C., *Adv. Mater.* **2017,** *29* (28), 1606491.

(23) (a) Shockley, W.; Queisser, H. J., *J. Appl. Phys.* **1961,** *32* (3), 510-519; (b) Rühle, S., *Solar Energy* **2016,** *130*, 139-147.

(24) Würfel, P., Limitations on Energy Conversion in Solar Cells. In *Physics of Solar Cells*, Wiley-VCH Verlag GmbH: 2005; pp 137-153.

(25) Shockley–Queisser limit. Available at: https://en.wikipedia.org/wiki/Shockley%E2%80%93Queisser_limit (Accessed 27 February 2018).

(26) (a) Debije, M. G.; Verbunt, P. P. C., *Adv. Energy Mater.* **2012,** *2* (1), 12-35; (b) Klampaftis, E.; Ross, D.; McIntosh, K. R.; Richards, B. S., *Sol. Energy Mater. Sol. Cells* **2009,** *93* (8), 1182-1194.

(27) van Sark, W. G.; Barnham, K. W. J.; Slooff, L. H., *Opt. Express* **2008,** *16* (26), 21773-21792.

(28) Shurcliff, W. A., *J. Opt. Soc. Am.* **1951,** *41* (3), 209.

(29) Weber, W. H.; Lambe, J., *Appl. Opt.* **1976,** *15* (10), 2299-300.

(30) Swartz, B. A.; Cole, T.; Zewail, A. H., *Opt. Lett.* **1977,** *1* (2), 73-5.

(31) Banal, J. L.; Zhang, B.; Jones, D. J.; Ghiggino, K. P.; Wong, W. W., *Acc. Chem. Res.* **2017,** *50* (1), 49-57.

(32) (a) Xu, J.; Zhang, B.; Jansen, M.; Goerigk, L.; Wong, W. W. H.; Ritchie, C., *Angew. Chem. Int. Ed.* **2017,** *56* (44), 13882-13886; (b) Zhang, B.; Soleimaninejad, H.; Jones, D. J.; White, J. M.; Ghiggino, K. P.; Smith, T. A.; Wong, W. W. H., *Chem. Mater.* **2017,** *29* (19), 8395-8403; (c) Banal, J. L.; Soleimaninejad, H.; Jradi, F. M.; Liu, M.; White, J. M.; Blakers, A. W.; Cooper, M. W.; Jones, D. J.; Ghiggino, K. P.; Marder, S. R.; Smith, T. A.; Wong, W. W. H., *J. Phys. Chem. C* **2016,** *120* (24), 12952-12958.

(33) (a) Gutierrez, G. D.; Coropceanu, I.; Bawendi, M. G.; Swager, T. M., *Adv. Mater.* **2016,** *28* (3), 497-501; (b) Meinardi, F.; McDaniel, H.; Carulli, F.; Colombo, A.; Velizhanin, K. A.; Makarov, N. S.; Simonutti, R.; Klimov, V. I.; Brovelli, S., *Nature Nanotechnology* **2015,** *10* (10), 878-885.

(34) (a) Shi, J.; Chang, N.; Li, C.; Mei, J.; Deng, C.; Luo, X.; Liu, Z.; Bo, Z.; Dong, Y. Q.; Tang, B. Z., *Chem. Commun.* **2012,** *48* (86), 10675-7; (b) Banal, J. L.; Ghiggino, K. P.; Wong, W. W., *Phys. Chem. Chem. Phys.* **2014,** *16* (46), 25358-63.

(35) Iasilli, G.; Battisti, A.; Tantussi, F.; Fuso, F.; Allegrini, M.; Ruggeri, G.; Pucci, A., *Macromol. Chem. Phys.* **2014,** *215* (6), 499-506.

(36) Banal, J. L.; White, J. M.; Ghiggino, K. P.; Wong, W. W., *Sci. Rep.* **2014,** *4*, 4635.

(37) De Nisi, F.; Francischello, R.; Battisti, A.; Panniello, A.; Fanizza, E.; Striccoli, M.; Gu, X.; Leung, N. L. C.; Tang, B. Z.; Pucci, A., *Mater. Chem. Front.* **2017,** *1* (7), 1406-1412.

(38) (a) Valeur, B.; Berberan-Santos, M., *Molecular fluorescence: principles and applications*. John Wiley & Sons: 2012; (b) Minei, P.; Fanizza, E.; Rodríguez, A. M.; Muñoz-García, A. B.; Cimino, P.; Pavone, M.; Pucci, A., *RSC Adv.* **2016,** *6* (21), 17474-17482.

(39) (a) Lucarelli, J.; Lessi, M.; Manzini, C.; Minei, P.; Bellina, F.; Pucci, A., *Dyes Pigm.* **2016,** *135*, 154-162; (b) Carlotti, M.; Fanizza, E.; Panniello, A.; Pucci, A., *Solar Energy* **2015,** *119*, 452-460.

(40) Mori, R.; Iasilli, G.; Lessi, M.; Muñoz-García, A. B.; Pavone, M.; Bellina, F.; Pucci, A., *Polym. Chem.* **2018**.

(41) (a) Hu, R.; Gomez-Duran, C. F.; Lam, J. W.; Belmonte-Vazquez, J. L.; Deng, C.; Chen, S.; Ye, R.; Pena-Cabrera, E.; Zhong, Y.; Wong, K. S.; Tang, B. Z., *Chem. Commun.* **2012,** *48* (81), 10099-101; (b) Chen, S.; Liu, J.; Liu, Y.; Su, H.; Hong, Y.; Jim, C. K. W.; Kwok, R. T. K.; Zhao, N.; Qin, W.; Lam, J. W. Y.; Wong, K. S.; Tang, B. Z., *Chem. Sci.* **2012,** *3* (6), 1804-1809; (c) Zhang, J.; Chen, R.; Zhu, Z.; Adachi, C.; Zhang, X.; Lee, C. S., *ACS Appl. Mater. Interfaces* **2015,** *7* (47), 26266-74.

(42) Banal, J. L.; White, J. M.; Lam, T. W.; Blakers, A. W.; Ghiggino, K. P.; Wong, W. W. H., *Adv. Energy Mater.* **2015,** *5* (19), 1500818.

(43) Zhu, M.; Zhuo, Y.; Cai, K.; Guo, H.; Yang, F., *Dyes Pigm.* **2017,** *147*, 343-349.

(44) (a) Zhao, Q.; Zhang, X. A.; Wei, Q.; Wang, J.; Shen, X. Y.; Qin, A.; Sun, J. Z.; Tang, B. Z., *Chem. Commun.* **2012,** *48* (95), 11671-3; (b) Zhao, Q.; Zhang, S.; Liu, Y.; Mei, J.; Chen, S.; Lu, P.; Qin, A.; Ma, Y.; Sun, J. Z.; Tang, B. Z., *J. Mater. Chem.* **2012,** *22* (15), 7387-7394.

(45) Currie, M. J.; Mapel, J. K.; Heidel, T. D.; Goffri, S.; Baldo, M. A., *Science* **2008,** *321* (5886), 226-8.

(46) Zhang, B.; Banal, J. L.; Jones, D. J.; Tang, B. Z.; Ghiggino, K. P.; Wong, W. W. H., *Mater. Chem. Front.* **2018**, *2*, 615-619.

(47) de Wild, J.; Meijerink, A.; Rath, J. K.; van Sark, W. G. J. H. M.; Schropp, R. E. I., *Energy Environ. Sci.* **2011,** *4* (12), 4835-4848.

(48) Monguzzi, A.; Frigoli, M.; Larpent, C.; Tubino, R.; Meinardi, F., *Adv. Funct. Mater.* **2012,** *22* (1), 139-143.

(49) Zhou, J.; Liu, Q.; Feng, W.; Sun, Y.; Li, F., *Chem. Rev.* **2015,** *115* (1), 395-465.

(50) Baluschev, S.; Yakutkin, V.; Miteva, T.; Wegner, G.; Roberts, T.; Nelles, G.; Yasuda, A.; Chernov, S.; Aleshchenkov, S.; Cheprakov, A., *New J. Phys.* **2008,** *10* (1), 013007.

(51) McCusker, C. E.; Castellano, F. N., *Top. Curr. Chem.* **2016,** *374* (2), 19.

(52) Schulze, T. F.; Schmidt, T. W., *Energy Environ. Sci.* **2015,** *8* (1), 103-125.

(53) Simon, Y. C.; Weder, C., *J. Mater. Chem.* **2012,** *22* (39), 20817-20830.

(54) Duan, P.; Yanai, N.; Kurashige, Y.; Kimizuka, N., *Angew. Chem. Int. Ed.* **2015,** *54* (26), 7544-9.

(55) Duan, P.; Asthana, D.; Nakashima, T.; Kawai, T.; Yanai, N.; Kimizuka, N., *Faraday Discuss.* **2017,** *196*, 305-316.

(56) Li, L.; Zeng, Y.; Yu, T.; Chen, J.; Yang, G.; Li, Y., *ChemSusChem* **2017,** *10* (22), 4610-4615.